FOI
SWEDISH DEFENCE
RESEARCH AGENCY

FOI-R--0412--SE
Feb 2002
ISSN 1650-1942
Technical report

Lingfu Zeng and Robin Olsson

Buckling-induced delamination analysis of composite laminates with soft-inclusion

Aeronautics Division, FFA
SE-172 90 Stockholm
Sweden

SWEDISH DEFENCE RESEARCH AGENCY

Aeronautics Division, FFA
SE-172 90 Stockholm
Sweden

FOI-R--0412--SE

Feb 2002

ISSN 1650-1942

Technical report

Lingfu Zeng and Robin Olsson

Buckling-induced delamination analysis of composite laminates with soft-inclusion

Issuing organization	Report number, ISRN	Report type
FOI – Swedish Defence Research Agency Aeronautics Division, FFA SE-172 90 Stockholm Sweden	FOI-R--0412--SE	Technical report
	Research area code 7. Vehicles	
	Month year Feb 2002	**Project no.** E824570
	Customers code 5. Contracted Research	
	Sub area code 72. Aeronautical Systems	

Author/s (editor/s)	Project manager
Lingfu Zeng Robin Olsson	Robin Olsson
	Approved by Anders Blom, Head, Strucures and Materials Deptartment
	Scientifically and technically responsible Börje Andersson

Report title

Buckling-induced delamination analysis of composite laminates with soft-inclusion

Abstract (not more than 200 words)

In this paper, the effect of material impact damage on buckling-driven delamination growth in composite laminates under compression is studied using a finite element method. The initial material damage, e.g. fibre fracture and matrix cracking due to impact, is modeled through a so-called soft-inclusion, in which an area with reduced stiffness is introduced in the analysis of buckling-induced delamaination growth with an ADINA-based finite element program. Parametric studies are carried out through numerical tests with different inclusion sizes and stiffness reductions, and a comparison with experiments is made. It is found that for single delaminations of moderate size, even significant stiffness reductions in one half of the delamination diameter have a fairly small influence on the initiation of delamination growth. Moreover, the experimentally measured local buckling load and deflection responses during delamination growth are lower than those predicted by the finite element model with severe stiffness reduction. It is concluded that such a soft-inclusion model is not sufficiently accurate to model the material damage, and more mathematically elaborated models which are capable to cope with material degradation, multiple delamination, crack closure and so on, should be developed.

Keywords

Composite laminate, material damage, buckling, delamination growth, finite element, shell, soft-inclusion

Further bibliographic information	Language English
ISSN 1650-1942	**Pages** 34 p.
	Price acc. to pricelist **Security classification: Open**

Utgivare	Rapportnummer, ISRN	Klassificering
Totalförsvarets Forskningsinstitut - FOI Avdelningen för flygteknik, FFA 172 90 Stockholm	FOI-R--0412--SE	Teknisk rapport
	Forskningsområde 7. Bemannade och obemannade farkoster	
	Månad, år Feb 2002	**Projektnummer** E824570
	Verksamhetsgren 5. Uppdragsfinansierad verksamhet	
	Delområde 72. Flygsystem	

Författare/redaktör	Projektledare
Lingfu Zeng Robin Olsson	Robin Olsson
	Godkänd av Anders Blom Institutionschef, Struktrur- och materialteknik
	Tekniskt och/eller vetenskapligt ansvarig Börje Andersson

Rapportens titel (i översättning)

Bucklingsdriven delamineringsanalys av kompositlaminat med mjuk inneslutning

Sammanfattning (högst 200 ord)

I denna rapport används en finit elementmetod för att studera effekten av skador i materialet på bucklingsdriven delamineringstillväxt i tryckbelastade kompositlaminat. Den initiella skadan i materialet, t ex fiberbrott och matrixsprickor pga slag, modelleras med en så kallad mjuk inneslutning, där en area med reducerad styvhet är införd vid analys av bucklingsdriven delamineringstillväxt med ett ADINA-baserat finit elementprogram. Parameterstudier utförs genom numeriska experiment med inneslutningar av olika storlek och styvhet, och en jämförelse med experimentella resultat är genomförd. Det visas att för enkeldelamineringar av måttlig storlek har även kraftiga styvhetssänkningar i halva delamineringsdiametern en relativt liten effekt på initieringen av delamineringstillväxt. Vidare observeras att de lokala bucklingslaster och utböjningar under delamineringstillväxt som uppmätts experimentellt är lägre än de som predikterats av den finita elementmodellen med en kraftigt reducerad styvhet. Det konstateras att en sådan modell med mjuk inneslutning icke är tillräckligt noggrann för att modellera skador i materialet, och mera matematiskt genomtänkta modeller, som är kapabla att hantera materialdegradering, multipeldelamineringar, sprickslutning m.m., måste utvecklas.

Nyckelord

Kompositlaminat, materiell skada, buckling, delamineringstillväxt, finit element, skal, mjuk inneslutning

Övriga bibliografiska uppgifter	Språk Engelska
ISSN 1650-1942	**Antal sidor:** 34 s.
Distribution enligt missiv	**Pris: Enligt prislista** **Sekretess: Öppen**

Contents

1. Introduction

Impact damage is a major concern in the design of aircraft structures of composite laminates as it often severely reduces the strength and stability performance of the structure [1]. Typically, impact damage zones contain matrix cracks between the fibers of a ply and delaminations between plies. Extensive impact damage can also results in fiber fracture. Furthermore, an impact damage causes normally multiple delaminations through the thickness of a laminate. The distribution of multiple delaminations depends in general on several factors, such as the laminate span-to-thickness ratio and the severity of the damage [2]. As buckling and post-buckling behavior of thin-walled structures of shell-type are severely sensitive to any imperfection, impact damage in composite laminates can therefore be expected to drastically change the behavior of buckling-driven delamination, both the initiation and growth. This, in turn, reduces the load-carrying capability of the structure.

Strength reductions are usually observed to be the most critical for structures loaded in compression [1]. These reductions are normally associated with buckling induced-delamination growth, which has been the subject of extensive research for two decades [3-5]. The studies have progressed from local buckling and growth initiation of one- and two-dimensional delaminations to simulation of growth without and with global buckling interaction [6-10]. The presence of fibers frequently constrains the cracks to interlaminar crack growth (delaminations), which generally occurs under mixed mode conditions [5]. Mixed mode fracture is caused both by anisotropy and by the combination of bending and stretching during buckling. The interlaminar toughness of composites is strongly dependent on the loading mode [11], which necessitates a reliable mode separation technique, as well as the use of reliable mixed mode growth criteria.

Extensive fractographical studies demonstrate that fiber fracture often is present in the impact damage zones of concern in certification of a composite structure [2]. Such damage causes significant local stiffness reductions, which may affect buckling and cause in-plane failure due to stress concentrations. Stiffness reductions of about 80 % in tension and 50 % in compression have been demonstrated on small coupons cut from impact damaged zones [12]. Experiments with panels having damage zones of equal size indicate that decreasing buckling loads are associated with increasing degrees of fiber damage [13]. Comparisons between impacted and artificially delaminated specimens have demonstrated that both types fail by buckling induced delamination growth [14]. The

impacted panel did, however, fail at a lower load. These results demonstrate that phenomena such as fiber fracture, multiple delaminations and initial imperfections need to be included in analysis models when simulating realistic impact damage.

The present work deals with analysis of the effect of material damage within the delamination area on buckling and buckling-induced delamination growth. Based on the fractographical observations in Refs. 2, 12-17, the material damage is modeled as a so-called soft-inclusion, as suggested in e.g. Ref. 2. In the modeling, a central zone with considerable fiber breakage is incorporated in the numerical model as a material with reduced stiffness, i.e. soft-inclusion. The size of the soft-inclusion zone is assumed to be less than half of the delamination size. Numerical tests are made using an in-house finite element program for simulation of buckling induced growth of single delaminations, DEBUGS [18].

The paper is organized as follows: In Section 2, the program DEBUGS and its theoretical background are briefly reviewed. In Section 3, the material impact damage modeling with soft-inclusion is described. In Section 4, numerical tests are first presented and parametric studies are carried through to quantitatively estimate the effect of impact damage. Thereafter, a comparison with experimental results is carried out. Finally in Section 5, concluding remarks are given.

2. Program system DEBUGS

DEBUGS is a program system developed specifically for simulation of buckling and buckling-induced interlaminar crack growth in composite laminate panels. It uses ADINA, a general-purpose commercial program provided by ADINA R&D, Inc., USA, as a primary solver, together with a set of external specialized modules for coping with crack growth with a so-called *r*-adaptive algorithm. This *r*-adaptive algorithm allows a remeshing during the course of delamination growth, such that the discretization follows with the development of delamination crack front. The remeshing is done through keeping the finite element topology unchanged, but relocating nodes when necessary.

In this section, the theoretical background and its numerical implementation into DEBUGS are briefly outlined. For a more detailed description, we refer to Refs. 8, 9 and 19, in particular, Nilsson and Giannakopoulos [19], and references therein.

2.1 Kinematical and constitutive modeling

The laminate composite panel under consideration consists of a plate with a thickness $t+T$, in which a single in-plane delamination of a smooth but otherwise arbitrary front Γ_D, enclosing a delaminated domain Ω_D, is initially embedded at depth t. The thickness of the delaminated member and the total thickness of the plate are assumed to be small as compared to other dimensions of the panel.

The panel is modeled by two plates, i.e. upper and lower plates, with mid-surfaces at $x_3 = t/2$ and $x_3 = -T/2$, respectively, see a one-dimensional sketch in Fig.1. Both the upper and lower plates are assumed to follow Reissner-Mindlin assumptions, *i.e.*

$$u_\alpha(x_1,x_2,z) = \bar{u}_\alpha(x_1,x_2) + z\theta_\alpha(x_1,x_2) \quad (1)$$

$$u_3(x_1,x_2,z) = \bar{u}_\alpha(x_1,x_2) \quad (2)$$

where the subscripts 1 and 2 refer to in-plane quantities, the subscript 3 to quantities in the direction normal to the mid-surface, and z is the distance from the mid-surface, respectively. Greek indices run from 1 to 2 and θ_α denotes the rotation of a transverse material fiber. An overbar refers to the quantities associated with the mid-surface.

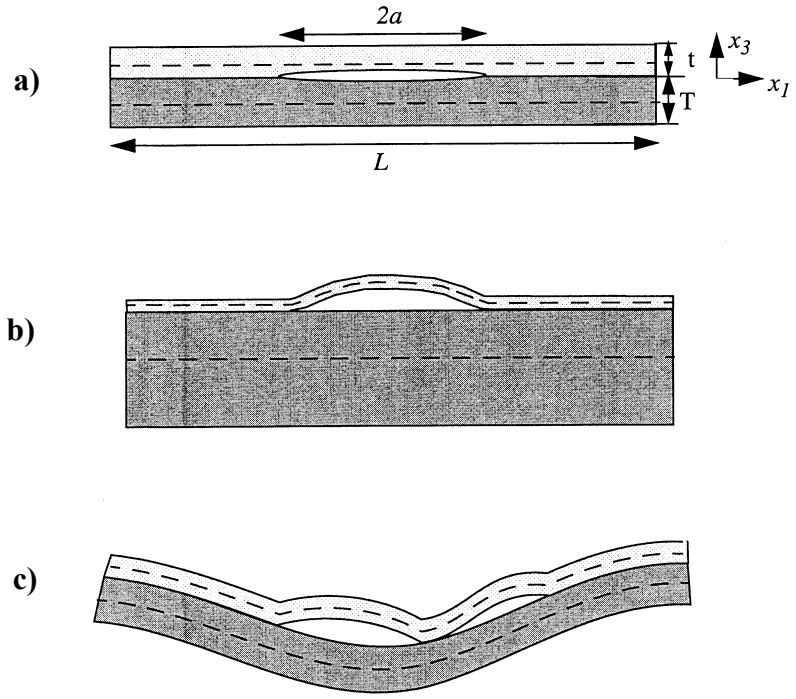

Fig. 1 Composite panel with an artificial delamination in one-dimension. a) Undeformed panel; b) Deformed panel when thin film condition assumed for the lower-plate; and c) Deformed panel when global bending allowed.

Small strains and moderate rotations are assumed. Hence, the strain tensor is defined as follows

$$e_{\alpha\beta} = e^0_{\alpha\beta} + z\kappa_{\alpha\beta} \tag{3}$$

$$e_{3\alpha} = (\overline{u}_{3,a} + \theta_\alpha)/2 \tag{4}$$

where the membrane strain tensor $e_{\alpha\beta}$ is given by

$$e^0_{\alpha\beta} = (\overline{u}_{\alpha,\beta} + \overline{u}_{\beta,\alpha} + \overline{u}_{3,\alpha}\overline{u}_{3,\beta})/2 \tag{5}$$

and $\kappa_{\alpha\beta}$ is the curvature tensor given by

$$\kappa_{\alpha\beta} = (\theta_{a,\beta} + \theta_{\beta,\alpha})/2 \tag{6}$$

The generalized sectional forces conjugate to the membrane strain and curvature tensors are given for elastic plates by

$$N_{\alpha\beta} = \partial W/\partial e^0_{\alpha\beta}\ , \quad M_{\alpha\beta} = \partial W/\partial \kappa_{\alpha\beta}\ , \quad Q_\alpha = \partial W/(2\partial e_{3\alpha}) \tag{7}$$

where W is the strain energy function.

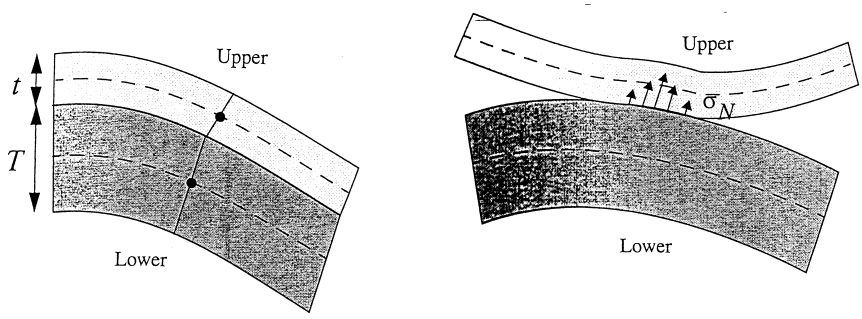

Fig. 2 Illustration of the structural model for an undelaminated domain (left) and a delaminated domain with contact (right).

In the *un-delaminated domain* the displacement continuity is prescribed along the 'interface' as illustrated in Figure 2, with rigid constraints linking the upper and lower plates, i.e.

$$\bar{u}_\alpha^{(U)} - \frac{t}{2}\theta_\alpha^{(U)} = \bar{u}_\alpha^{(L)} - \frac{T}{2}\theta_\alpha^{(L)} \tag{8a}$$

$$\bar{u}_3^{(U)} = \bar{u}_3^{(L)} \tag{8b}$$

where $u^{(U)}$ and $u^{(L)}$ denote the displacements of upper- and lower-plates.

In the *delaminated domain* a contact condition is enforced as follows

$$\sigma_N = S\frac{2d}{T+t} \quad \text{for} \quad d < 0 \tag{9a}$$

$$\sigma_N = 0 \quad \text{for} \quad d \geq 0 \tag{9b}$$

$$d = \left\| (\bar{x}_i^{(U)} + \bar{u}_i^{(U)}) - (\bar{x}_i^{(L)} + \bar{u}_i^{(L)}) \right\|_{l_2} - (\frac{T+t}{2}) \tag{9c}$$

where σ_N denotes the resulting contact pressure, d the elongation of a line segment linking two points of a contact pair on the mid-surfaces of the upper- and lower-plates with initially identical in-plane coordinates, see also Fig. 2, and S a selected transverse stiffness, respectively. The contact pressure becomes non-zero when the distance between two points of a contact-pair in the upper and lower plate is less than their initial distance. The conditions (9a,b,c) assume that the out-of-plane components of the relative displacements are substantially larger than those of the in-plane components.

The constraint conditions (9a,b,c) introduces an additional nonlinearity to the problem. The contact region as well as the contact pressure for a given load are determined by an iterative procedure with the following convergence criteria

$$\sum_{i=1}^{N-N_c}\left(1-\frac{d_i}{|d_i|}\right)\le \varepsilon_d \tag{9d}$$

$$\sum_{i=1}^{N-N_c}\left(1-\frac{R_i}{|R_i|}\right)\le \varepsilon_R \tag{9e}$$

where ε_d and ε_R denote the associated convergence tolerances, N is the number of nodes in the delaminated region and N_c the number of nodes with active contact springs, respectively. N_c is unknown and must be determined iteratively for a given load.

2.2 Energy release rate and delamination growth

Linear elastic fracture mechanics will be used as the base for modeling of delamination growth. Hence, energy release rates and stress intensity factors are parameters to be determined along the crack front Γ_D during a loading process. The total energy release rate at local crack growth G can be computed as the discontinuity in field variables across the crack front of an energy momentum tensor P_{nn}

$$G=\left\|P_{nn}\right\| \tag{10}$$

where $\|x\|$ denote the "jump" of variable x across the crack front, see Figure 3(a).

The energy momentum tensor can be written as follows

$$P_{nn}=W-N_{n\alpha}\overline{u}_{a,n}-Q_n\overline{u}_{3,n}-M_{n\alpha}\theta_{\alpha,n} \tag{11}$$

where n is the direction normal to the crack front. This expression was first derived by Storåkers and Andersson [20] for von Karman's nonlinear plate theory and later extended to Reissner-Mindlin plate theory by Nilsson and Storåkers [21].

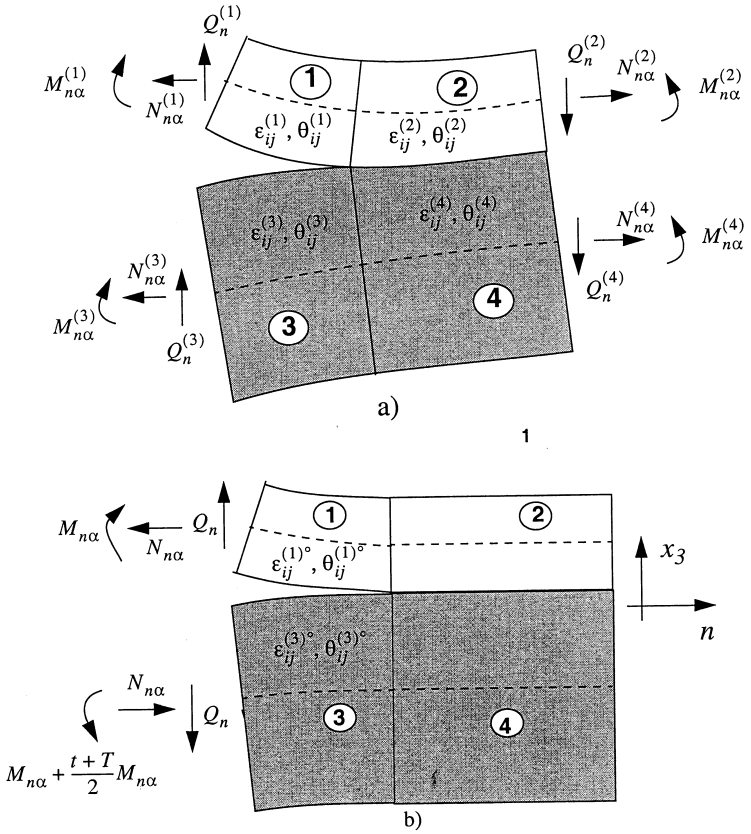

Fig. 3 Split beam element with section forces prior to superposition (upper) and after superposition (lower).

The nonlinear plate problem may locally be approximated by a "linear beam" problem by superposing a homogeneous strain field such that the undelaminated region becomes undeformed. Referring to Fig. 3 and the notations defined in the figure we have

$$\varepsilon_{ij}^{(h)^\circ} = \varepsilon_{ij}^{(h)} + \varepsilon_{ij}^{(h+1)} \qquad \text{for } h = 1,3 \tag{12a}$$

$$\theta_{ij}^{(h)^\circ} = \theta_{ij}^{(h)} + \theta_{ij}^{(h+1)} \qquad \text{for } h = 1,3 \tag{12b}$$

$$\theta_{ij}^{(h)^\circ} = \varepsilon_{ij}^{(h)} \equiv 0 \qquad \text{for } h = 2,4 \tag{12c}$$

and from the equilibrium

$$N_{n\alpha}^{(3)^\circ} = N_{n\alpha}^{(1)^\circ} \tag{13a}$$

$$M_{n\alpha}^{(3)^\circ} = M_{n\alpha}^{(1)^\circ} + N_{n\alpha}^{(1)^\circ} \frac{t+T}{2} \tag{13b}$$

$$Q_n^{(3)^\circ} = Q_n^{(1)^\circ} \tag{13c}$$

where the superscript "o" denote corresponding variables after the superposition. Hence, the number of unknown variables can be reduced to 5, i.e. $(N_{n\alpha}, M_{n\alpha}, Q_n)$ and Eq. (11) can be reformulated in terms of the "beam-sectional forces" after the superposition as follows

$$P_{nn}^{(h)^\circ} = \frac{1}{2}\left(N_{nn}^{(h)^\circ} \varepsilon_{nn}^{(h)^\circ} + N_{nt}^{(h)^\circ} \varepsilon_{nt}^{(h)^\circ} + M_{nn}^{(h)^\circ} \kappa_{nn}^{(h)^\circ} + Q_n^{(h)^\circ} \varepsilon_{3n}^{(h)^\circ} \right) \qquad (14)$$

for the upper plate (h=1) and the lower plate (h=3), where the subscript t is the tangential direction. The total energy release rate at local crack growth G can then be computed by

$$G = \left\| P_{nn} \right\| = P_{nn}^{(1)^\circ} + P_{nn}^{(3)^\circ} \qquad (15)$$

Delamination growth takes place when the energy release rate G reaches the critical fracture toughness G_c. Experiments show that the critical fracture toughness depends strongly on the relative amount of the fundamental fracture modes. The mode-dependent fracture toughness $G_c(\Psi)$ may be expressed as

$$G_c(\Psi) = G_{IC} f(\Psi) \qquad (16)$$

where G_{Ic} is a reference critical fracture toughness for curve-fitting, see e.g. Nilsson et al. [19], $f(\psi)$ a function describing the mixed mode-dependency, and ψ is the phase angle defined by

$$\Psi = \arctan(K_{II} / K_I) \qquad (17)$$

where K_I and K_{II} are stress intensity factors for the modes I and II, respectively. In DEBUGS an approximate fracture mode separation is performed. The mode separation is based on an assumption that the stress intensity factors vary linearly with the sectional force resultants.

2.3 Failure criteria

In the current version of DEBUGS, the composite material is limited to be isotropic or anisotropic linear elastic. To predict the onset of material damage in a complex stress state, e.g. fibre breakage and/or matrix cracking, Hashin's failure criteria for composite materials can be used.

Assuming that fibers are aligned with the first material principal direction, *a*-direction, thus making the material transversely isotropic about *a*-direction, the Hashin criteria reads as follows:

$$\tau_a^2 / X_t^2 + \left(\tau_{ab}^2 + \tau_{ac}^2\right) / S_{ab}^2 \geq 1 \qquad \text{for } \tau_a > 0 \tag{18a}$$

$$\tau_a^2 / X_c^2 \geq 1 \qquad \text{for } \tau_a < 0 \tag{18b}$$

$$(\tau_b + \tau_c)^2 / Y_t^2 + \left(\tau_{bc}^2 - \tau_b \tau_c\right) / S_{tr}^2 + \left(\tau_{ab}^2 + \tau_{ac}^2\right) / S_{ab}^2 \geq 1 \qquad \text{for } (\tau_b + \tau_c) > 0 \tag{18c}$$

$$\begin{aligned}&(\tau_b + \tau_c)\left[1 - Y_c^2 / (2S_{tr})^2\right] / Y_c + (\tau_b + \tau_c)^2 / (2S_{tr})^2 + \\ &+\left(\tau_{bc}^2 - \tau_b \tau_c\right) / S_{tr}^2 + \left(\tau_{ab}^2 + \tau_{ac}^2\right) / S_{ab}^2 \geq 1 \qquad \text{for } (\tau_b + \tau_c) < 0\end{aligned} \tag{18d}$$

where X_t and X_c are the tensile and compressive ply strengths in the fiber direction, i.e. *a*-direction, Y_t and Y_c are the tensile and compressive ply strengths in the direction perpendicular to the fibers, or *b*-direction, and S_{ab} and S_{tr} are the shear strengths on the *a*-*b* plane (in-plane of ply) and on *b*-*c* plane (out-of-plane of ply), τ with various subscript are stress components, respectively.

In equations (18), four types of failure are defined: tensile fiber failure (18a), compressive fiber failure (18b), tensile matrix failure (18c) and compressive failure (18c). Failure will initiate when any of these conditions is violated.

3. Soft-inclusion modeling of impact damage

Experiments show that the impact of polymer matrix composites often leads to matrix cracking, delamination and fiber breakage. The damage structure can be very complex and depends on several factors, such as ply layup, type of impact and so on. It has, however, been found that fiber breakage is fairly uniform through the thickness and concentrates to a small region, say less than one half of delamination width, see Fig. 4 from [2].

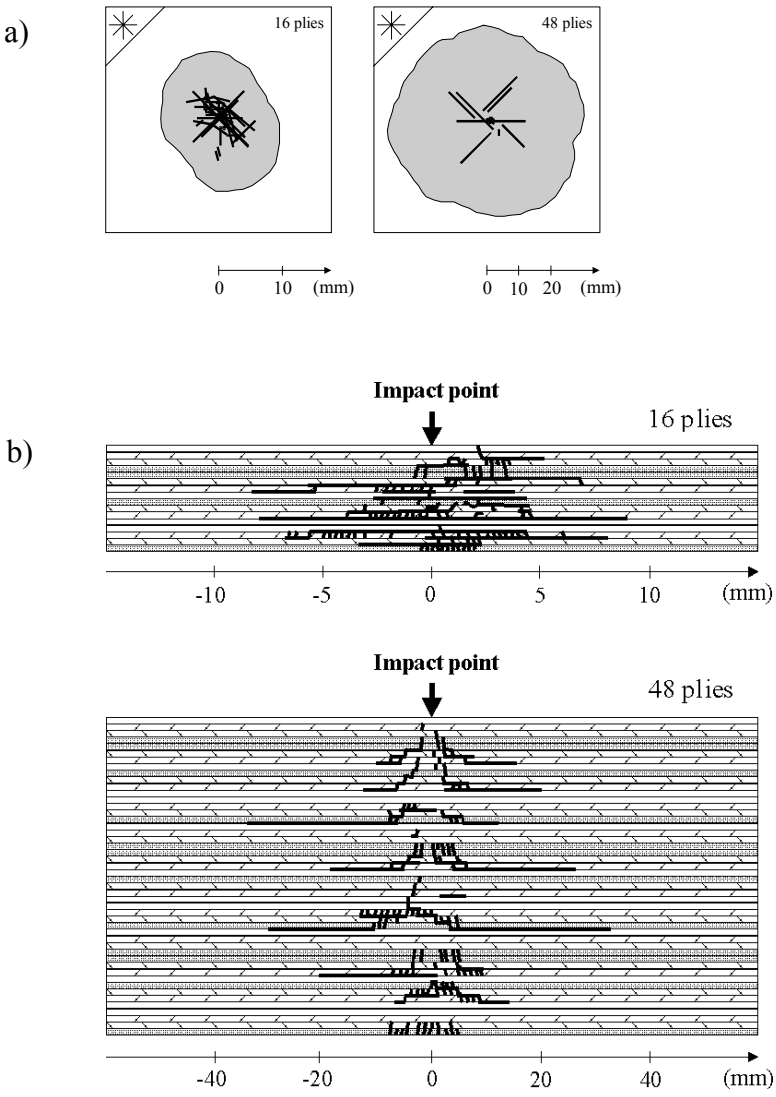

Fig. 4 Fiber breakage and delamination (a) and matrix cracking and delamination (b) observed in a typical impact damage test

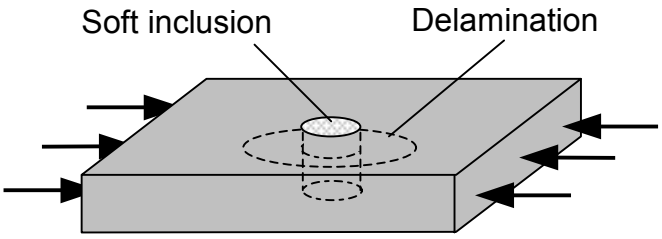

Fig. 5 Soft-inclusion modeling of material impact damage

Based on these observations, it has been suggested, see e.g. Sjögren et al. [12], that impact damage may be modeled through a so-called soft inclusion, i.e. by incorporation of a small region within the delamination area, where reduced material stiffness, e.g. elastic moduli of plies, is used, see Fig. 5.

Such a modeling concept is not new and has been used in many other engineering applications in connection with empirical design or calculations using handbooks or so. In our attempt, a circular area with radius R is created in the middle of the initially delaminated area, see Figs. 1 and 8, such that different elastic moduli can be assigned to elements in this area. In the following presentation, the relative stiffness inclusion, ξ, is introduced such that the elastic moduli used in this circular area, E_{soft}, are given by

$$E_{\text{soft}} = \xi E_{undamaged} \tag{19}$$

where $E_{undamaged}$ is the elastic moduli of the undamaged composite laminate. Parametric studies will be carried below with varying ξ and R.

4. Numerical tests

The influence of a soft inclusion is studied through a series of finite element analyses of a test specimen of which various laboratory test results are available. The test case has also earlier been analyzed with the previous version of DEBUGS.

4.1 Test specimen

The test specimen considered is a composite laminate panel of 150x 150x4.55 mm cross-ply laminate with the loaded edges clamped and the unloaded edges free. In Fig. 6, the test setup is shown. Based on previous FE-studies [9] a free length of 154 mm was used in the model to account for the flexibility of the end clamps. The 35 ply layup is $(90º/0º)_{17}/90º$, where the 0º coincides with the load direction. The ply thickness is 0.130 mm. This specimen type has been tested with 30 mm radius artificial delamination [9, 14] and with 30 J impact damage [14]. The panels were made of Hexcel HTA/6376C carbon/epoxy prepared with the ply properties in compression given in Tab. 1 and failure stresses for Hashin's criteria given in Tab. 2.

Tab. 1 Elastic constants of plies in compression

E_{11}	E_{22}=E_{33}	G_{12}=G_{13}	G_{23}	ν_{12}=ν_{13}	ν_{23}
131 GPa	11.7 GPa	5.2 GPa	3.9 GPa	0.30	

Note: $\nu_{ji} = \nu_{ij} E_{jj} / E_{ii}$ for orthotropic material

Tab. 2 Failure stresses for Hashin's criteria [MPa]

σ_{B11}		σ_{B22}		τ_{B12}	τ_{B13}=τ_{B23}
Tension	Compr.	Tension	Compr.	Shear	Shear
2090	1720	112	346	131	131

The impacted specimens contained delaminations in an elliptical region with axis lengths 58x30mm, where the minor axis coincides with the load direction. Delamination growth usually initiated in the third interface from the surface. For simplicity all modeling was done using a circular delamination with radius 30 mm. The fiber damage of these specimens was not measured but previous studies of similar specimens with the layup $(0^o/90^o)_{17}/0^o$ have shown fiber damage in all plies within a 30x17 mm central region [15]. We note that in Fig. 6 the length 154 mm is used to account for the flexibility of the end clamps and the length of the laboratory test specimen is 150 mm.

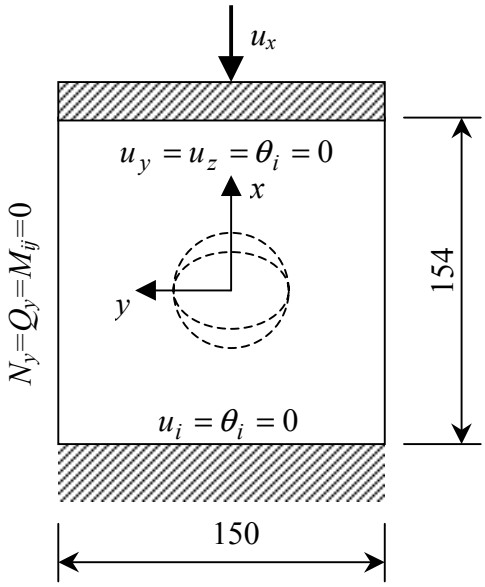

Fig. 6 Compression test of a composite laminate panel

4.2 Numerical tests

Numerical tests on the composite laminate panel described in the previous section are carried using DEBUGS with several different relative stiffness inclusion alternatives, ξ=25%, 50%, 75% and 100%, and with soft-inclusion sizes R=7.5 mm and R=15 mm, respectively. In Fig. 7, the finite element mesh used for all analyses and the local buckling mode for R=15mm and ξ=50% are shown. In the next section, part of the analysis results will be given and discussed.

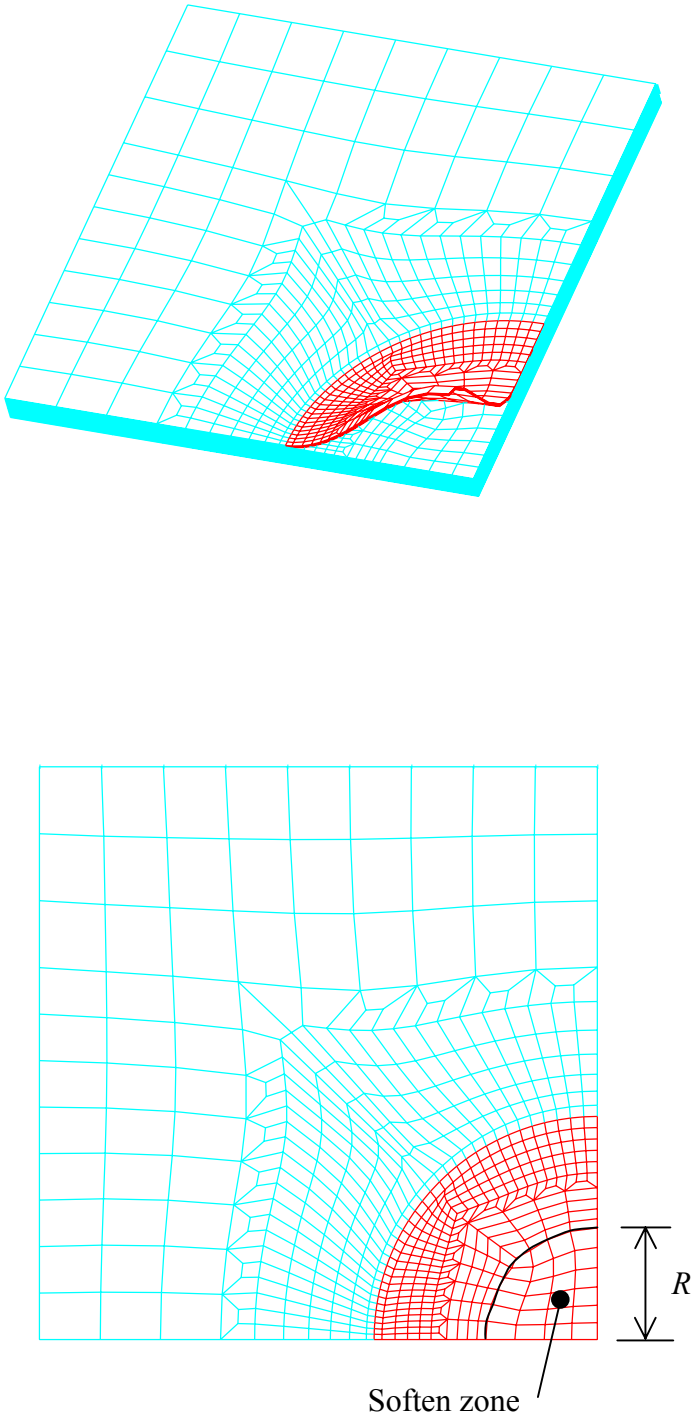

Fig. 7 Finite element mesh (lower) and the local buckling mode (uppe) for the soft-inclusion alternative ξ=50% and R=15mm.

4.3 Parametric studies

In this section, parametric studies will be carried out and the effect of the stiffness reduction degree (R,ξ) on the buckling and buckling-driven delamination growth will be studied.

In Fig. 8 load-deflection relations for cases with a circular delamination of radius 30 mm, and a soft-inclusion radius R=15 mm, with relative stiffness inclusions ξ=25%, 50% and 100%, are plotted. The onset loads for delamination growth have been indicated by triangles on the vertical axis through the center. It is noted that the local and global buckling load decreases with decreasing stiffness of the soft inclusion. It is shown from the figure that the delamination growth onset is more or less coincident with global buckling, which is only moderately affected by a reduced inclusion stiffness.

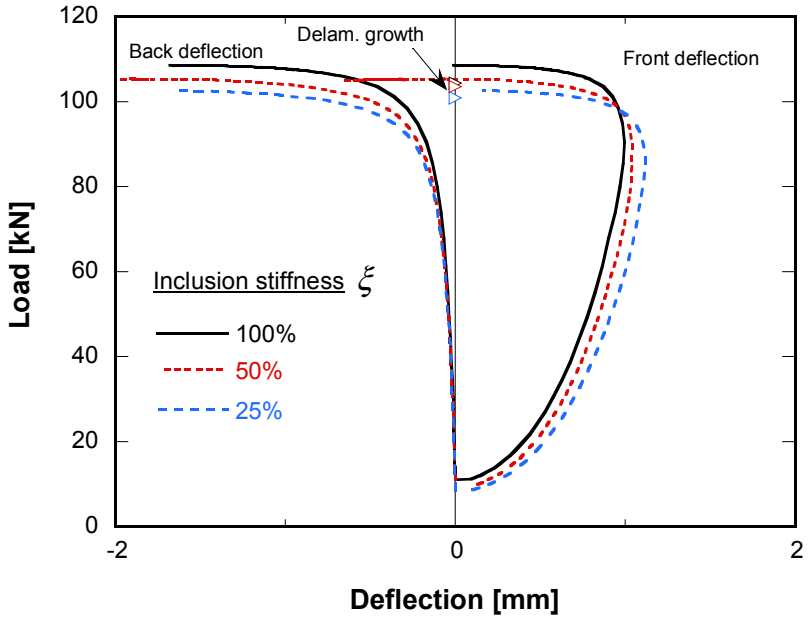

Fig. 8 Load-deflection curves at the center of the panel obtained with varying inclusion stiffness for inclusion size R=15 mm

In Fig. 9 load-deflection relations for cases with a circular delamination of radius 30 mm, and a relative stiffness inclusion ξ=50% for two different soft-inclusion sizes. It is shown in the figure that the effect of increasing inclusion size R is moderate and similar to the effect obtained when reducing the inclusion stiffness.

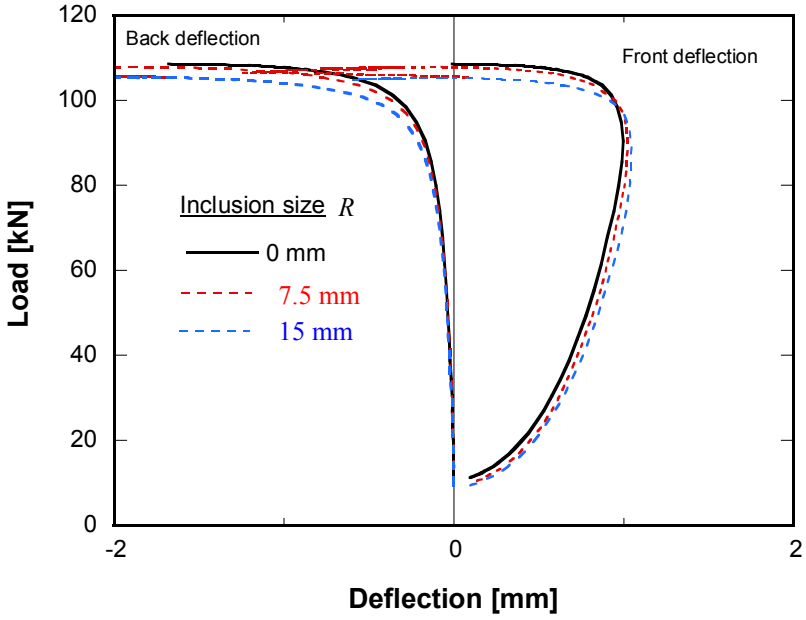

Fig. 9 Load-deflection curves at the center of the panel obtained with varying inclusion size for inclusion stiffness ξ=50%

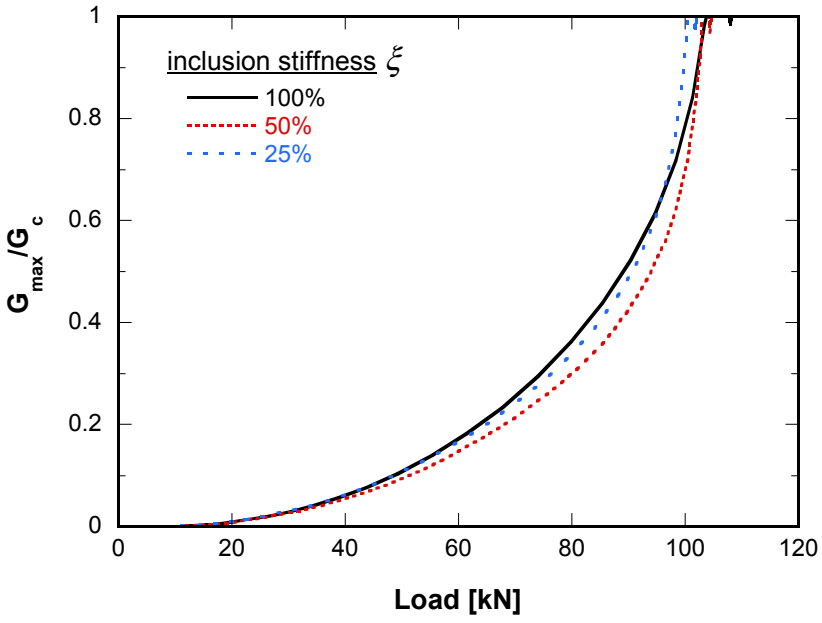

Fig. 10 Normalized maximum strain energy release rates v.s. the compression load with varying inclusion stiffness for inclusion size R=15 mm

In Fig. 10, the normalized maximum strain energy release rate G_{max}/G_c as a function of load are plotted for different values of the relative inclusion stiffness when simulating the delamination growth. It is shown that the value increases gradually after local buckling and increases steeply at the global buckling load, as observed in previous studies. It may be concluded that the relative inclusion stiffness ξ affects both the global buckling load and onset load for delamination growth moderately in a similar way.

In Fig. 11 the effect of inclusion stiffness on delamination growth is studied for different soft-inclusion stiffnesses. It shows that the delamination growth becomes more or less unstable as soon as the global buckling load has been reached, at least for the present geometry, which lacks post-buckling stiffness. Moreover, the influence of the relative inclusion stiffness ξ is small and apparently directly related to the reduction in global buckling load.

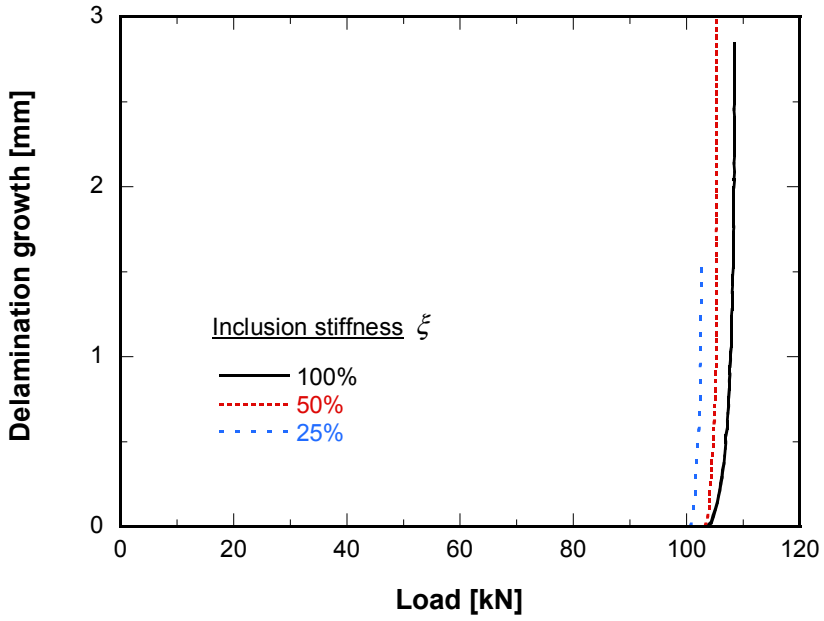

Fig. 11 The effect of relative inclusion stiffness ξ on delamination growth for inclusion size R=15 mm

In Fig. 12 the applied average strains, i.e. the applied displacement divided by the specimen length, at the stage when the local delamination buckling occurs, are studied for different stiffness inclusions. The buckling strain of a circular sublaminate clamped along its boundary

seems to be dependent only on the thickness-to-radius ratio. However, reduced inclusion stiffness reduces the corresponding local buckling stress, which must be in equilibrium with stresses in the surrounding material. Thus, reduced inclusion stiffness corresponds to a lower applied stress and strain in the surrounding material.

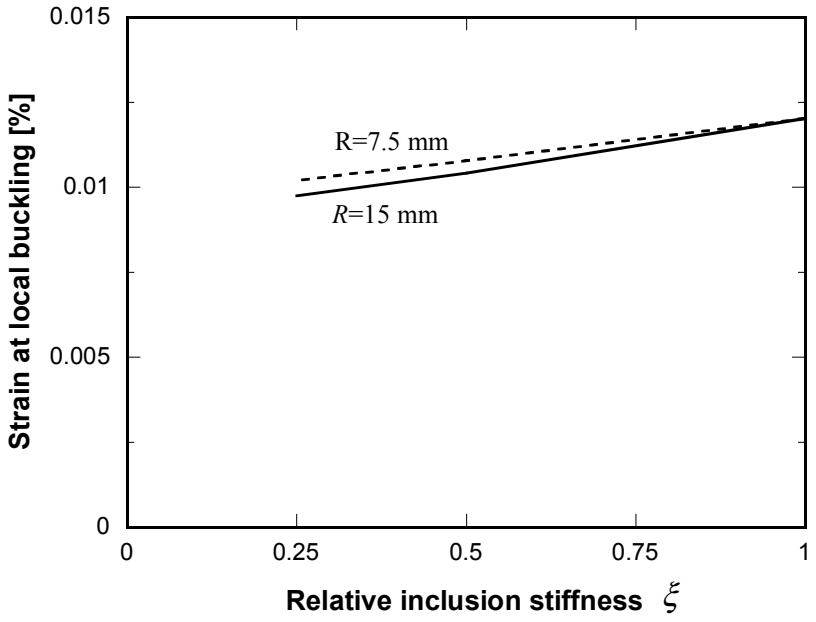

Fig. 12 The effect of soft-inclusion of the local delamination buckling

In Fig. 13 the effect of the soft-inclusion stiffness on the global buckling behavior is studied. The nominal strain at global buckling was found to be independent of the size and stiffness of the inclusion. Figure 13 shows the loss in global buckling load, which is more or less proportional to the stiffness reduction of the section with the inclusion. This observation may be appreciated by noting that global buckling essentially is identical to the buckling of a wide Euler beam. Thus, the inclusion merely corresponds to a loss of the effective beam area.

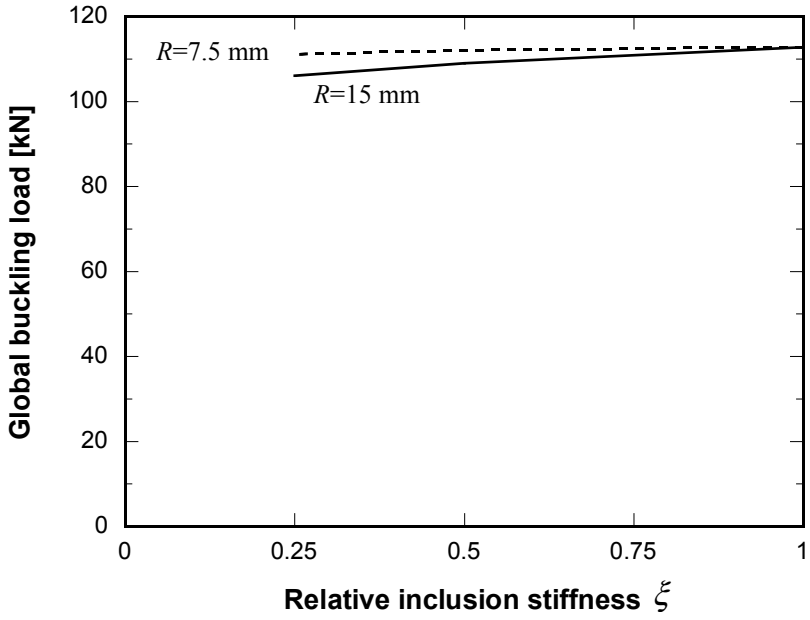

Fig. 13 The effect of soft-inclusion on the global buckling behavior

4.4 Comparison with experiments

In Fig. 14 a comparison between the finite element analysis and experiments is made for cases with a soft-inclusion R=15 mm and ξ= 25%. We note that the assumed *inclusion size is at the upper limit* of the size 30 x 17 mm observed from fractography [15], and that the *assumed stiffness inclusion is lower* than the 50% reduction obtained in previous compression tests on regions with fiber fracture [12]. In spite of this the failure load of the impacted panel is significantly lower than predicted. It should be noted that finite element results have shown a good agreement with tests with artificial single delaminations. Furthermore, it may be noted that the local buckling is fairly insignificant in the impacted panel. In fact, it was hardly detectable in the remaining two impacted panels [14].

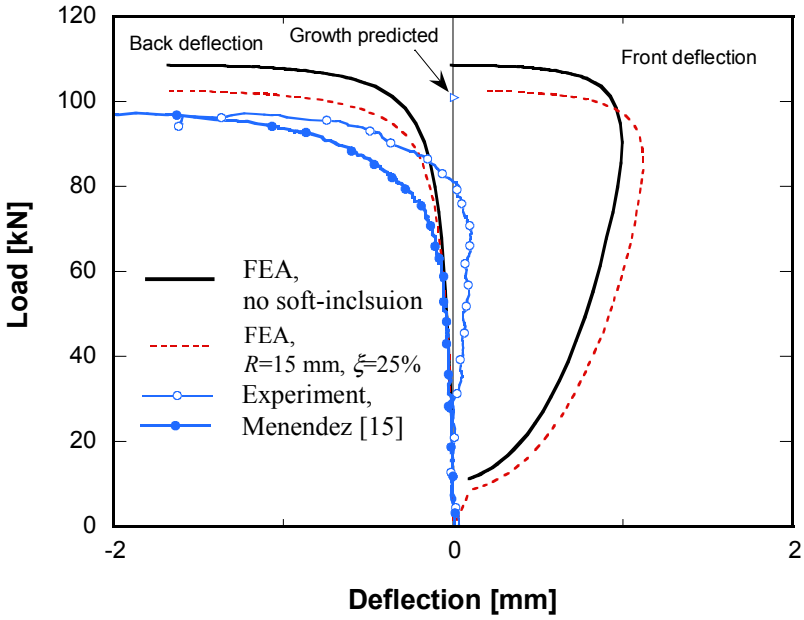

Fig. 14 Load-deflection curves at the center of the composite panel. Finite element analysis v.s. experiments

It can be seen from Fig. 14 that the finite element analysis, with or without soft-inclusion, seems to only provide a quantitatively meaningful estimate for the load-carrying capacity. A rather big discrepancy exists in the deflection response during the whole loading process. This is not an unexpected phenomenon. Soon as the local buckling initiates, fibers and matrices in the delaminating region exhibit a significantly complex behavior, implying that linear elasticity and a direct treatment of continua are no more valid for materials in that region. It is evident that a proper modeling of impact damage must include additional features, such as material nonlinearity, initial imperfections and multiple delaminations. It should be noted that "in-phase" buckling of multiple delaminations with an initial imperfection might act as a severe structural softening of the damage region. Such a buckling behavior has previously been observed in compression tests on impacted panels [17]. Another possible explanation for insignificant local buckling may be nonlinear material behavior due closure of cracks with fiber fracture.

4.5 Failure prediction

As the delamination growth occurs, the material damage will progress and an evolution of the damage will take place during loading. The damage progress and evolution can not be modeled in the current simulation using DEBUGS. In Fig. 15 failure areas predicted using Hashin's failure criteria are plotted for a soft-inclusion case ξ=50% and R=15mm, at a stage when 166 crack growth increments are made. The figure shows the failure on the bottom and top layer, both 90° to loading, of the thin sublaminate above the delaminated region. A closer study of the results revealed that both plies fail by matrix compressive failure, while no fiber fracture is predicted. Thus, differences in failure regions of the top and bottom plies reflect the shift in the position of peak compressive strain, associated with the local buckling shape. Similarly, the regions with equal failure in both plies indicate regions with negligible bending in the loading direction. It may be concluded that growth of the softened region due to the progress of fiber damage is unlikely to happen in the present case. Matrix cracks will, however, occur but do not present a site for ply jumping in the direction of delamination growth.

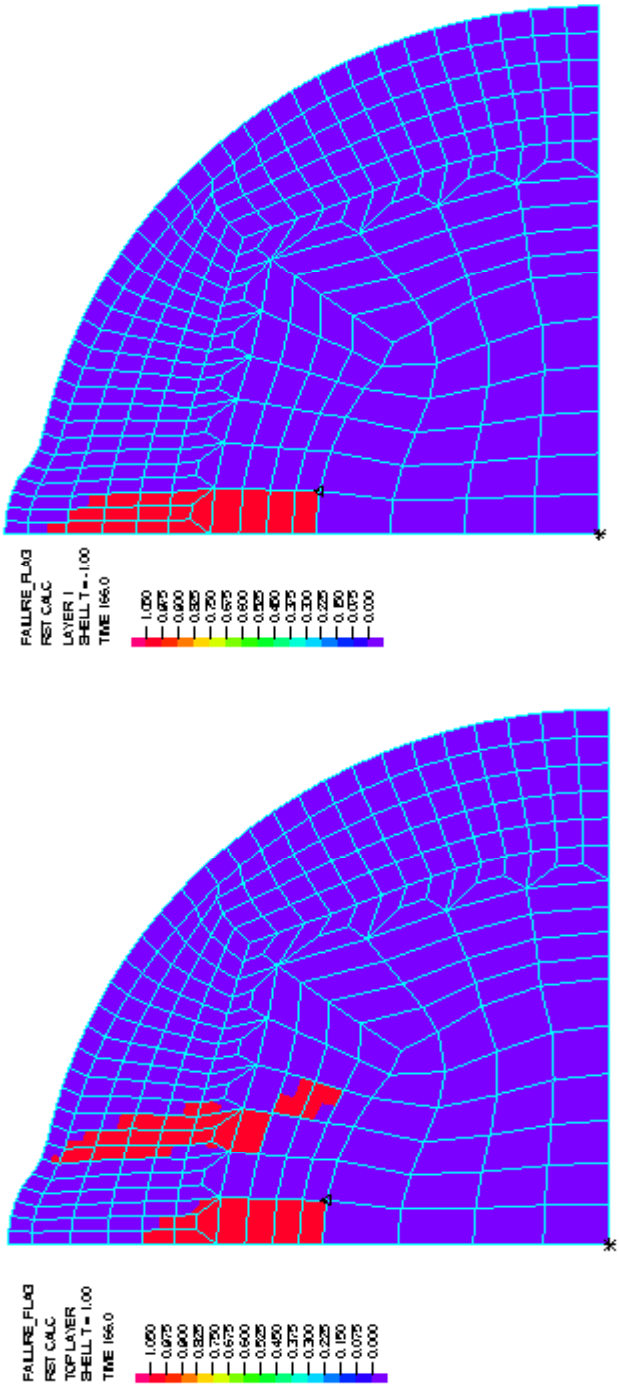

Fig. 15 Failure regions predicted according to Hanshin's criteria in the bottom (upper) and top (lower) plies of the locally buckled sublaminate.

5. Concluding remarks

In this paper, the effect of material impact damage on buckling-driven delamination growth in composite laminates under compression is studied numerically. The initial material damage, e.g. fibre fracture and matrix cracking due to impact, is modeled through a soft-inclusion, in which an area with reduced stiffness is introduced in buckling-driven delamination analysis of the composite laminates using an ADINA-based program system DEBUGS. Such a modeling concept is definitively not new and could be found in many engineering applications many years ago in connection with empirical design or calculations using handbooks or so. Nevertheless, it is worthwhile to incorporate such a possibility into DEBUGS.

The numerical tests and parametric studies made in this report have been focused on a simple, uni-axially loaded panel. It is found that for single delaminations of moderate size, even significant stiffness reductions in one half of the delamination diameter have a fairly small influence on the initiation of delamination growth. Moreover, the local buckling load and deflection responses during delamination growth, predicted by the finite element model with severely stiffness reduction, are observed to be higher than observed experimentally. It is concluded that such a soft-inclusion model is not sufficiently accurate to model the material damage, more mathematically elaborated models which are able to cope with material degradation, multiple delamination, crack closure and so on, should be developed.

Acknowledgements

The work reported in the paper was funded by The Swedish Defence Materiel Administration (FMV), which is gratefully acknowledged.

References

1. Abrate S. (1991), Impact on laminated composite materials, *Appl. Mech. Rev*., 44:155-189.

2. Sjögren, A. (1999), Fractographic characterization of impact damage in carbon fiber/epoxy laminates, *FFA TN 1999-17*, The Aeron. Res. Inst. of Sweden, Bromma.

3. Krishna Murty, A.V. and Reddy, J.N. (1993), Compressive failure of laminates and delamination buckling: a review, *Shock Vibr. Digest* 25(3)3-12.

4. Bolotin, V.V. (1996), Delaminations in composite structures: its origin, buckling, growth and stability, *Composites Part B* 27B(2) 129-145.

5. Hutchinson, J.W. and Suo, Z. (1992), Mixed mode cracking in layered materials, *Advances Appl. Mech.* 29, 63-191.

6. Chai, H., Babcock, C.D. and Knauss, W.G. (1981), One-dimensional modelling of failure in laminated plates by delamination buckling, *Int. J. Solids Struct.* 17(11)1069-1083.

7. Chai, H. and Babcock, C.D. (1985), Two-dimensional modelling of failure in delaminated laminates, *J. Compos. Mater.* 19(1)67-98.

8. Nilsson, K.-F., Thesken, J.C, Sindelar, P., Giannakopoulos A.E. and Storåkers, B. (1993), A theoretical and experimental investigation of buckling induced delamination growth, *J. Mech. Phys. Solids* 41(4)749-782.

9. Nilsson, K.-F., Asp, L.E., Alpman, J. and Nystedt, L. (2001), Delamination buckling and growth for delaminations at different depths in a slender composite panel, *Int. J. Solids Struct.* 38(17)3039-3071.

10. Nilsson, K.-F., Asp, L.E. and Sjögren, A. (2001), On transition of delamination growth behaviour for compression loaded composite panels, *Int. J. Solids Struct.* 38(46-47)8407-8440.

11. Olsson, R., Thesken, J.C., Brandt, F. Jönsson, N. and Nilsson, S. (1996), Investigations of delamination criticality and the transferability of growth criteria, *Compos. Struct*. 36(3/4)221-247.

12. Sjögren, A., Krasnikovs, Y. and Varna, J. (1999), Experimental determination of elastic properties of impact damage in carbon fibre/epoxy laminates, *Composites* Part A 32(9)1237-1242.

13. Olsson, R. (1999), A review of impact experiments at FFA during 1986 to 1998, FFA TN 1999-08, The Aeron. Res. Inst. of Sweden, Bromma.

14. Asp, L.E., Nilsson, S. and Singh, S. (1999), An experimental investigation of the influence of delamination growth on the residual strength of impacted laminates *Composites Part A* 32(9)1229-1235.

15. Menendez A. E. (1998), Characterization of impact damage in composite laminates, *FFA TN 1998-24*, The Aeron. Res. Inst. of Sweden, Bromma.

16. Nilsson, S. (2000), Compression tests on impacted rectangular composite laminates with various lay-ups, *FFA TN 2000-02*, The Aeron. Res. Inst. of Sweden, Bromma.

17. Melin, L.G. and Schön, J. (2001), Buckling behaviour and delamination growth in impacted composite specimens under fatigue load: an experimental study, *Compos. Sci.Techn.* 61(13)1841-1852.

18. Zeng, L (2001), User's Manual for DEBUGS 2.0 - A finite element prgram for delamination buckling and growth simulation of laminate composite pannels, Technical Report, *FOI-R--0239--SE*, Swedish Defence Research Agency, Sweden.

19. Nilsson, K.-F. and Giannakopoulos, A. (1995), A finite element analysis of configurational stability and finite growth of buckling driven delamination, *J. Mech. Phys. Solids*, 43, 1983-2021.

20. Storåkers, B. and Andersson, B. (1988), Nonlinear plate theory applied to delamination in composites, *J. Mech. Phys. Solids*, 36, 689-718.

21. Nilsson, K.-F. and Storåkers, B. (1992), On the interface crack growth in composite plates, *J. Appl. Mech*., 59, 530-538.

22. ADINA R&D Inc (1997), *User's Manual, Theory and Modelling guide*, Vol. I, 118-120.